Inorganic Chemistry

Article

pubs.acs.org/IC

DFT Study of the Stereoselective Formation of *cis*-$W(CO)_4(\eta^2\text{-}C_2H_4)_2$ in the Gas-Phase Consecutive Coordination of C_2H_4 onto Doubly Coordinatively Unsaturated $W(CO)_4$

Yo-ichi Ishikawa,* Kei Umemoto, and Arifumi Okada

Department of Chemistry and Materials Technology, Kyoto Institute of Technology, Matsugasaki, Sakyo-ku, Kyoto 606-8585, Japan

Supporting Information

ABSTRACT: B3LYP-based density functional theory (DFT) calculations are reported that provide insight into the stereoselective formation of *cis*-$W(CO)_4(\eta^2\text{-}C_2H_4)_2$ observed in the pulsed 266 nm laser photolysis of tungsten hexacarbonyl ($W(CO)_6$) in the presence of C_2H_4 in the gas phase at room temperature (*J. Phys. Chem.* **1995**, *99*, 4558). $W(CO)_4(\eta^2\text{-}C_2H_4)$ formed through the coordination of C_2H_4 onto coordinatively unsaturated $W(CO)_4$ was found to have a pseudo-C_{2v} symmetry (distorted trigonal bipyramid with an angle of ca. 90° between the two equatorial COs) with a bond dissociation enthalpy (BDE) of $W-C_2H_4$ of 125 kJ mol^{-1}. In the subsequent coordination of C_2H_4 onto the $W(CO)_4(\eta^2\text{-}C_2H_4)$, having one vacant coordinatively unsaturated site, no barrier was found in the reaction path to *cis*-complex formation, while there was a barrier of about 89 kJ mol^{-1} to the *trans*-complex. The calculations show that the stereoselective formation of *cis*-$W(CO)_4(\eta^2\text{-}C_2H_4)_2$ is due to kinetic rather than thermodynamic control. The *trans*-$W(CO)_4(\eta^2\text{-}C_2H_4)_2$ was calculated to be more stable than *cis*-$W(CO)_4(\eta^2\text{-}C_2H_4)_2$ by about 10 kJ mol^{-1}. The BDE of $W-C_2H_4$ in *cis*-$W(CO)_4(\eta^2\text{-}C_2H_4)_2$ was estimated to be 61 kJ mol^{-1}.

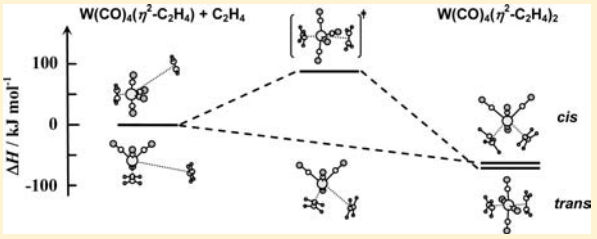

INTRODUCTION

In coordination chemistry, isomerization through ligand exchange is such a fundamental subject that many experimental and theoretical studies have been carried out from both thermodynamic and kinetic points of view.[1−11] For example, the axial−equatorial exchange in trigonal-bipyramidal (tbp) molecules has been interpreted by the so-called Berry pseudorotation mechanism (tbp-sp-tbp interconversion).[1] It is said that this exchange does not happen through dissociative or bimolecular processes but is an intramolecular process, suggesting that an activation barrier on the ground-state surface is low so that isomerization proceeds even at room temperature. Information about isomerization on ground-state surfaces is clearly relevant to understanding the stereochemistry of coordination compounds.[7]

For the disubstituted d^6 metal carbonyls $M(CO)_4(C_2H_4)_2$, two stereoisomers, *cis* and *trans*, are possible, which have been generally produced through replacement of carbonyl groups with C_2H_4 by UV photolysis of $M(CO)_6$ in the presence of C_2H_4. However, the isomer product distribution seems to depend strongly on photolysis conditions such as temperature, phase, and irradiation method (pulsed or continuous). The continuous UV photolysis of $M(CO)_6$ in the presence of C_2H_4 in the condensed phase has generally produced both isomers, though the *cis*-isomer might be occasionally missed owing to its instability.[2,3] The selective formation of *trans*-$Cr(CO)_4(C_2H_4)_2$ in the continuous UV photolysis of the mixture of $Cr(CO)_6$/C_2H_4 in alkane at low temperature[4] has been interpreted by the secondary photoisomerization of *cis*-$Cr(CO)_4(C_2H_4)_2$ to *trans*-$Cr(CO)_4(C_2H_4)_2$ and the lability of *cis*-$Cr(CO)_4(C_2H_4)_2$. The primary reaction in the UV photolysis of $M(CO)_6/C_2H_4$ is proposed by Daniel and Veillard[11] to be the formation of $M(CO)_5(C_2H_4)$. This is followed by the elimination of a carbonyl ligand through the secondary excitation of $M(CO)_5(C_2H_4)$ into the ^1E ligand field state to form $M(CO)_4(C_2H_4)$ with C_2H_4 basal. Reaction of this species with C_2H_4 results in the $M(CO)_4(C_2H_4)_2$ with *cis* structure through the C_2H_4 coordination reaction. The photoisomerization of *cis*-$M(CO)_4(C_2H_4)_2$ to *trans*-$M(CO)_4(C_2H_4)_2$ has not been well discussed so far.

The pulsed UV photolysis of $Cr(CO)_5(C_2H_4)$ in the presence of C_2H_4 produced only *cis*-$Cr(CO)_4(C_2H_4)_2$, which was unstable and reacted with CO by dissociative substitution in the presence of CO and C_2H_4:[6]

$$cis\text{-}Cr(CO)_4(C_2H_4)_2 \rightarrow Cr(CO)_4(C_2H_4) + C_2H_4 \quad (1)$$

$$Cr(CO)_4(C_2H_4) + C_2H_4 \rightarrow cis\text{-}Cr(CO)_4(C_2H_4)_2 \quad (2)$$

$$Cr(CO)_4(C_2H_4) + CO \rightarrow Cr(CO)_5(C_2H_4) \quad (3)$$

The unimolecular decay constant of *cis*-$Cr(CO)_4(C_2H_4)_2$ was estimated to be $(6 \pm 2) \times 10^4$ s^{-1} at 295 K,[6] and the bond dissociation enthalpy (BDE) of $Cr-C_2H_4$ in *cis*-$Cr(CO)_4(C_2H_4)_2$ was reported to be ca. 60 kJ mol^{-1}.[3] These kinetic and thermodynamic properties seem to be consistent

Received: April 26, 2012
Published: October 25, 2012

   dx.doi.org/10.1021/ic300858d | *Inorg. Chem.* 2012, 51, 11365−11370

with the instability of *cis*-$M(CO)_4(C_2H_4)_2$ at room temperature. Our previous time-resolved infrared absorption measurement in the gas phase also suggested a stereoselective formation of *cis*-$W(CO)_4(\eta^2\text{-}C_2H_4)_2$ in a pulsed 266 nm laser photolysis of tungsten hexacarbonyl, $W(CO)_6$, in the presence of C_2H_4 at room temperature.[12]

In this study, we elucidate why only *cis*-$W(CO)_4(\eta^2\text{-}C_2H_4)_2$ was produced in the sequential coordination of two ethene ligands to $W(CO)_4$ at room temperature. The geometries of the relevant species ($W(CO)_4$, $W(CO)_4(\eta^2\text{-}C_2H_4)$, and $W(CO)_4(\eta^2\text{-}C_2H_4)_2$) were optimized using DFT calculations. The resultant vibrational frequencies were compared with the characteristic shifts in the C−O vibrational frequency observed using a transient infrared absorption spectroscopy.[12] The BDEs of W−(C_2H_4) in these complexes were also estimated. Potential energy surfaces (PES) were investigated for the ethene coordination and the isomerization in the ground singlet state of the tungsten carbonyl−ethene complexes.

COMPUTATIONAL METHODS

Hybrid DFT (B3LYP) calculations were used for all related tungsten−metal carbonyl compounds using the Gaussian 03W program.[13] A basis set composed of 6-311+G(2d,p) functions on hydrogen, carbon, and oxygen atoms and the LANL2DZ basis function with ECP on tungsten atom was used in combination with the B3LYP calculation. This combination was chosen because it gave a reasonable optimized structure and vibrational frequency results for the C−O stretching mode of transition-metal carbonyls ($M(CO)_n$; M = Cr, Mo, and W, n = 3−6)[14] and $W(CO)_5L$ (L = NH_3 and C_2H_4).[15] An appropriate, generally accepted correction was made for the calculated harmonic frequency (ω_{cal}) to estimate the theoretical fundamental frequency (ν_{corr}) by multiplying ω_{cal} with a scaling factor (λ = 0.9679).[16]

Bond dissociation enthalpies at 298 K (ΔH_{298}) were estimated using the following equation:

$$\Delta H_{298} = \Delta E_e + \Delta ZPE + \Delta E_{th} + \Delta(PV)$$

where ΔE_e is the difference in the optimized electronic energies between the reactant and product system, ΔZPE is the zero point energy correction estimated from the vibrational frequencies, ΔE_{th} is the thermal energy correction associated with the transnational, rotational, and vibrational energies between 0 and 298 K, and $\Delta(PV)$ is the molar work equal to ΔnRT.[17]

RESULTS AND DISCUSSION

C_2H_4 Complex Assignment. In the gas phase at room temperature, $W(CO)_4$ was observed to be almost selectively produced by a pulsed 266 nm laser photolysis of tungsten hexacarbonyl, $W(CO)_6$.[18]

$$W(CO)_6 + h\nu(266\ nm) \rightarrow W(CO)_4 + 2CO \quad (4)$$

The structure of $W(CO)_4$ has been discussed in detail in a previous paper.[14] DFT calculations showed that optimized $W(CO)_4$ adopts a C_{2v} structure (**40-A**) with the following structural parameters: $r(W-C_{ax})$ = 2.053 Å, $r(W-C_{eq})$ = 1.939 Å, $r(C_{ax}-O_{ax})$ = 1.145 Å, $r(C_{eq}-O_{eq})$ = 1.155 Å,

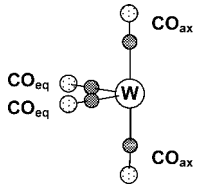

40-A

$\angle C_{ax}-W-C_{ax}$ = 179.8°, $\angle C_{eq}-W-C_{eq}$ = 88.89°, $\angle W-C_{ax}-O_{ax}$ = 177.6°, $\angle W-C_{eq}-O_{eq}$ = 179.8°, where "ax" is an abbreviation for axial position and "eq" for equatorial position, as shown in the above scheme. $W(CO)_4$ with a planar, nearly D_{4d} symmetry was estimated to be located 107 kJ mol^{-1} higher than the lowest ground state (**40-A**).

For the coordination reaction of C_2H_4 to doubly coordinatively unsaturated $W(CO)_4$ in the gas phase at room temperature, the following consecutive mechanism has been proposed based on time-resolved infrared spectroscopy:[12]

$$W(CO)_4 + C_2H_4 \rightarrow W(CO)_4(\eta^2\text{-}C_2H_4) \quad (5)$$

$$W(CO)_4(\eta^2\text{-}C_2H_4) + C_2H_4 \rightarrow W(CO)_4(\eta^2\text{-}C_2H_4)_2 \quad (6)$$

We therefore started this study with an investigation of the structure of $W(CO)_4(\eta^2\text{-}C_2H_4)$. For the singlet state of $W(CO)_4(\eta^2\text{-}C_2H_4)$, the three following structures were located at local minima on the potential energy surface using the B3LYP optimization:

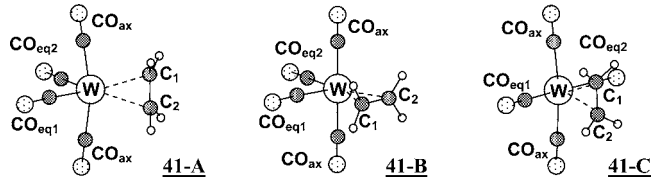

The electronic energy of **41-A** (distorted trigonal bipyramid, d-tbp) was calculated to be lower than that of **41-B** (square-pyramid with C_2H_4 basal, sp-basal) by 22 kJ mol^{-1} and than that of **41-C** (square-pyramid with C_2H_4 apical, sp-apical) by 68 kJ mol^{-1}. The BDEs for C_2H_4 dissociation in **41-A** and **41-B** were estimated to be 125 and 103 kJ mol^{-1}, respectively. The isomerization between the three species will be discussed later. The d-tbp structure with an angle of ca. 90° between the two equatorial carbonyl ligands was reported to be more stable than the other geometries (square pyramid or trigonal bipyramid) in the *ab initio* SCF calculation of $Mo(CO)_4(C_2H_4)$.[11] No other minimum energy structures could be found in the singlet ground state by the B3LYP calculations. The C═C bond length in the complexes was in the range 1.38−1.41 Å, longer than in a free C_2H_4, calculated by the same method as 1.326 Å (the experimental value is 1.337 Å[19]), suggesting the contribution of π-back-donation in the C_2H_4 coordination.

Figure 1 shows a comparison between the observed time-resolved infrared absorption spectra (ν_{obs})[12] and the corrected theoretical frequencies (ν_{corr}) of the CO-stretching modes of $W(CO)_4$ and $W(CO)_4(\eta^2\text{-}C_2H_4)$. In the calculated spectra, the height of each rectangle indicates the relative absorption intensity obtained from the calculations. The time-resolved infrared absorption spectra (TRIR) spectra in the 1890−2030 cm^{-1} range were observed following the 266 nm pulse laser photolysis of $W(CO)_6$ (~10 mTorr) in the presence of C_2H_4 (0.5 Torr) at 5.5 Torr of total pressure with balance Ar.[12] The early-time spectrum (a), obtained 0.6 μs after photolysis laser pulse, was mainly attributed to $W(CO)_4$, and the late-time spectrum (b), at 2.4 μs after, to $W(CO)_4(\eta^2\text{-}C_2H_4)$. For the early-time spectrum (a), the reasonable coincidence of the experimental and calculated spectra (ν_{obs} of $W(CO)_4$ and ν_{corr} of **40-A**) in both the C−O stretching frequencies and the relative peak intensities supports the selective production of $W(CO)_4$ following 266 nm photolysis. This spectrum (a) is also very similar to the spectrum of a "relaxed" $W(CO)_4$ observed following the 248 nm pulse photolysis of $W(CO)_6$ in the absence of C_2H_4.[20] For the late-time spectrum (b), the calculated infrared absorption pattern suggests the **41-A** structure for $W(CO)_4(\eta^2\text{-}C_2H_4)$ rather than the **41-B** or **41-**

dx.doi.org/10.1021/ic300858d | *Inorg. Chem.* 2012, 51, 11365−11370

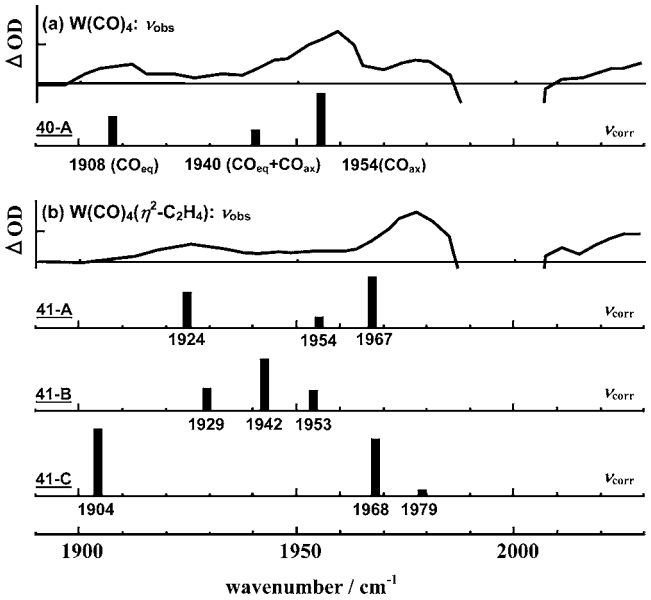

Figure 1. Comparison of the infrared difference absorption spectrum observed in the gas phase and the vibrational frequencies (ν_{corr}) calculated for $W(CO)_4$ (**40-A**) and $W(CO)_4(\eta^2\text{-}C_2H_4)$ (**41-A**, **41-B**, and **41-C**) represented as black rectangles. The height of each rectangle indicates the calculated relative absorption intensity. The ordinate scale, ΔOD, indicates the difference optical density between before irradiation and 0.6 μs (a) and 2.4 μs (b) after 266 nm pulse laser photolysis of the mixture of $W(CO)_6$ (~10 mTorr) and C_2H_4 (0.5 Torr) at a total pressure of 5.5 Torr with the balance Ar.

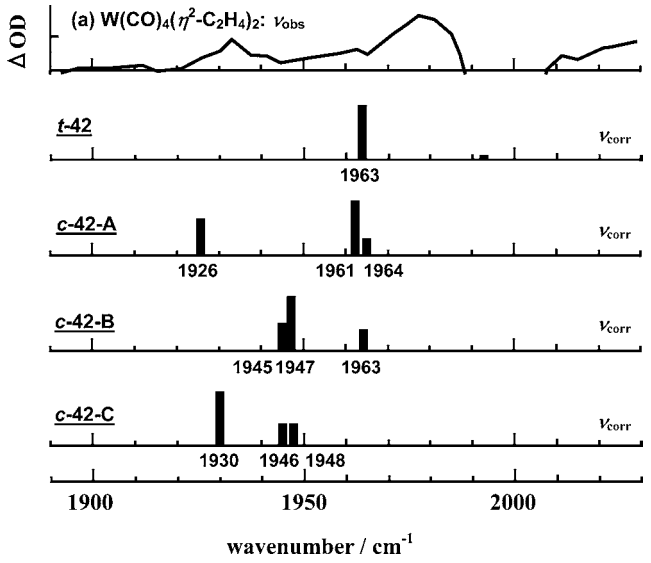

Figure 2. Comparison of the infrared difference absorption spectrum observed in the gas phase and the vibrational frequencies (ν_{corr}) calculated for *trans*-$W(CO)_4(\eta^2\text{-}C_2H_4)_2$ (***t*-42**) and *cis*-$W(CO)_4(\eta^2\text{-}C_2H_4)_2$ (***c*-42-A**, ***c*-42-B**, and ***c*-42-C**) represented as black rectangles. The height of each rectangle reflects the calculated relative absorption intensity. The ordinate scale, ΔOD, indicates the change in optical density between before irradiation and 7.2 μs after 266 nm pulse laser photolysis of a mixture of $W(CO)_6$ (~10 mTorr) and C_2H_4 (0.5 Torr) at a total pressure of 5.5 Torr with the balance Ar.

C structure. This assignment is reasonable from a thermodynamical point of view because the **41-A** is calculated to be more stable than the **41-B** and **41-C** by 22 and 68 kJ mol^{-1}, respectively.

DFT optimization trials were then carried out to elucidate the structure of the $W(CO)_4(\eta^2\text{-}C_2H_4)_2$ complex. Four stable structures were identified for the singlet state. These are shown below. Of them, *trans*-$W(CO)_4(\eta^2\text{-}C_2H_4)_2$ (***t*-42**) had the lowest energy.

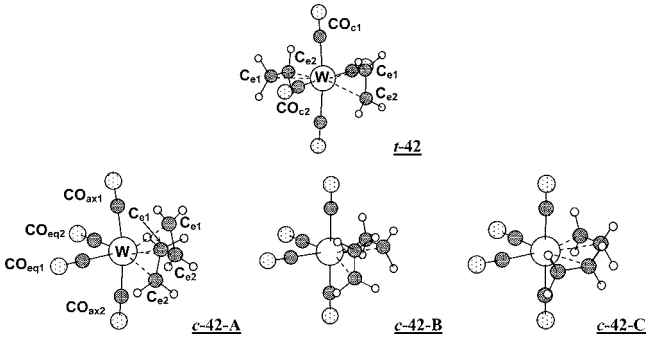

It was more stable than the *cis*-isomer, ***c*-42-A**, by about 11 kJ mol^{-1}. The ***c*-42-A** isomer was the most stable of the *cis*-isomers. It was lower in energy than the ***c*-42-B** and ***c*-42-C** structures by 2 and 11 kJ mol^{-1} in ΔH, respectively. The BDE for C_2H_4 dissociation from $W(CO)_4(\eta^2\text{-}C_2H_4)_2$ was estimated to be 61 kJ mol^{-1} in the case of ***c*-42-A** (→ **41-A** + C_2H_4) and 142 kJ mol^{-1} in the case of ***t*-42** (→ **41-C** + C_2H_4). This calculated BDE of ***c*-42-A** is consistent with the lability of $Cr(CO)_4(C_2H_4)_2$ at room temperature[6] and the experimental value of ca. 60 kJ mol^{-1} for the Cr complex.[3]

Figure 2 shows a comparison between the observed infrared absorption spectrum (ν_{obs})[12] and the corrected theoretical frequencies (ν_{corr}) of the CO-stretching modes of four optimized structures of $W(CO)_4(\eta^2\text{-}C_2H_4)_2$. The absorption spectrum (a) was observed at 7.2 μs after the photolysis laser pulse under the same experimental condition as Figure 1 and was assigned to $W(CO)_4(\eta^2\text{-}C_2H_4)_2$ from the kinetic analyses.[12] The observed spectrum is inconsistent with the formation of *trans*-$W(CO)_4(\eta^2\text{-}C_2H_4)_2$ (***t*-42**), which was projected to have only one CO stretching absorption peak, as confirmed in Figure 2. Taking into account the number of peaks and their intensity pattern, the absorption spectrum suggests that the product in the coordination reaction of C_2H_4 to $W(CO)_4(\eta^2\text{-}C_2H_4)$ (reaction 6) is the *cis*-isomer, ***c*-42-A**, even though the *trans*-form has been calculated to be more stable than the *cis*-one (***c*-42-A**) by about 11 kJ mol^{-1}. This implies the reaction is under kinetic control.

Reaction Paths of C_2H_4 Coordination to $W(CO)_4(\eta^2\text{-}C_2H_4)$. Calculated potential energy surfaces for the formation of *cis*- and *trans*-$W(CO)_4(\eta^2\text{-}C_2H_4)_2$ from $W(CO)_4(\eta^2\text{-}C_2H_4)$ + C_2H_4 reactions are shown in Figure 3. The selective formation of *cis*-$W(CO)_4(\eta^2\text{-}C_2H_4)_2$ through kinetic control is substantiated by the PES calculation results that show a substantial potential barrier of 89 kJ mol^{-1} for the formation of the *trans*-complex, while there is no barrier in the formation of the *cis*-complex. In the *trans*-complex formation path, there seems to be two distinct structural deformations in $W(CO)_4(\eta^2\text{-}C_2H_4)$. At first, the C_2H_4 in $W(CO)_4(\eta^2\text{-}C_2H_4)$ spins about 90° around the coordination axis. This is followed by an increase in the angle between the two equatorial CO ligands (α).

dx.doi.org/10.1021/ic300858d | *Inorg. Chem.* 2012, 51, 11365−11370

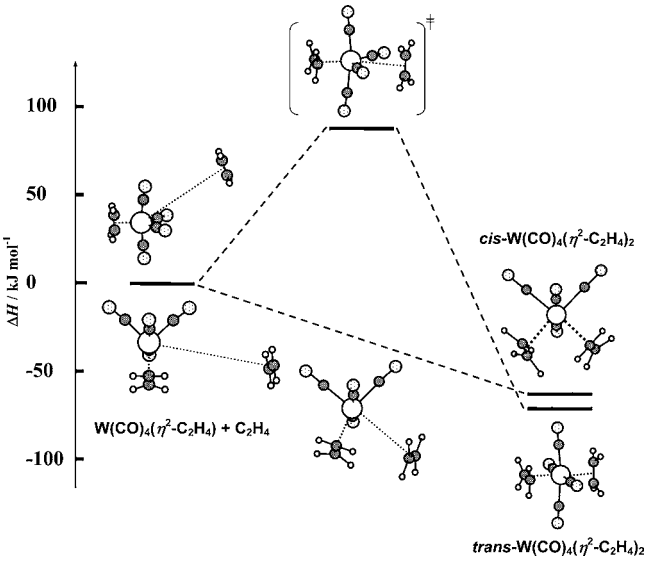

Figure 3. Schematic potential reaction surfaces for the formation of *cis*- and *trans*-$W(CO)_4(\eta^2\text{-}C_2H_4)_2$ from the reaction of $W(CO)_4(\eta^2\text{-}C_2H_4)$ with C_2H_4. The *trans*-isomer was more stable than the reactant system ($W(CO)_4(\eta^2\text{-}C_2H_4) + C_2H_4$) by 72 kJ mol^{-1} and than the *cis* isomer by 11 kJ mol^{-1}. The reaction barrier for the formation of the *trans*-isomer was calculated to be 89 kJ mol^{-1}.

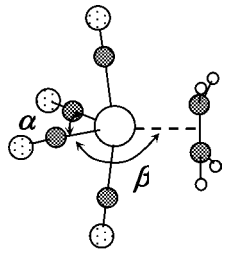

In the *cis*-complex formation path, the main deformation is a rotation of C_2H_4 around the CO_{ax}–W–CO_{ax} axis, corresponding to a decrease of one CO_{eq}–W–C_2H_4 angle (β). The energies required for these two main deformations were calculated as a function of angle (α and β) and are shown in Figure 4. All coordinates except α and β were optimized. In the case of β deformation, the optimization was carried out under the additional restriction that the C_2H_4 axis was perpendicular to a plane including W and two equatorial carbon atoms, and the center of C═C bond was included in the plane. In the α deformation two different conformations appear in the optimization, identified as *A*- and *B*-types in Figure 4a. The *A*-type conformation has an O–C–W angle less than 180°, similar to the lowest energy structure of $W(CO)_4(\eta^2\text{-}C_2H_4)$, and the *B*-type one has an angle larger than 180°. The *A*-type structures with $\alpha \geq 134°$ and the *B*-type structures with $\alpha \leq 134°$ had one imaginary frequency. The calculation indicates that the α deformation has a barrier of about 120 kJ mol^{-1}, suggesting that the high potential barrier of 89 kJ mol^{-1} found for the *trans*-complex formation is mainly due to the angle deformation of two equatorial carbonyls needed to accommodate the second C_2H_4 ligand in this conformation.

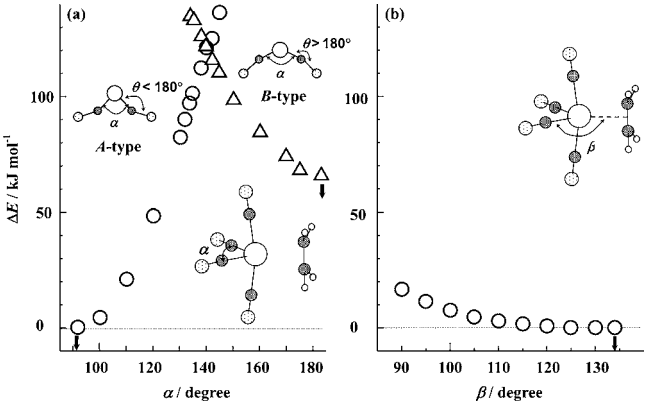

Figure 4. Angle deformation energy in $W(CO)_4(\eta^2\text{-}C_2H_4)$ as a function of the angle, α, between two equatorial carbonyls (a) and the angle, β, between C_2H_4 and one equatorial carbonyl (b). A down arrow indicates the angle of each fully optimized structure.

The C_2H_4 coordination reactions on $W(CO)_4(\eta^2\text{-}C_2H_4)$ were further analyzed using the activation strain model[21] in which activation energies ($\Delta E^{\ddagger}$) were decomposed into the activation strain ($\Delta E^{\ddagger}_{strain}$) of reactants and the stabilizing interaction energy ($\Delta E^{\ddagger}_{int}$) between the reactants in the activated complex in the transition state (TS): $\Delta E^{\ddagger} = \Delta E^{\ddagger}_{strain} + \Delta E^{\ddagger}_{int}$. In the formation of *trans*-$W(CO)_4(\eta^2\text{-}C_2H_4)_2$ with $\Delta E^{\ddagger}$ = 86 kJ mol^{-1}, the $\Delta E^{\ddagger}_{strain}$ of 92 kJ mol^{-1} was found to be much larger than the stabilizing interaction ($\Delta E^{\ddagger}_{int}$) of −6 kJ mol^{-1}. Both deformation and strain studies support the picture that the much higher barrier of *trans*-formation originates from steric deformation of the equatorial C–W–C angle in $W(CO)_4(\eta^2\text{-}C_2H_4)$. Before a favorable stabilizing interaction with C_2H_4 can occur, the angle must spread from ca. 90°, which causes the stabilizing interaction between the W center and C═C bond in the ethene coordination to contribute relatively late in the reaction. A similar strain analysis was not appropriate for *cis*-$W(CO)_4(\eta^2\text{-}C_2H_4)_2$ formation because there was no activation barrier. However the total strain energy of the $W(CO)_4(\eta^2\text{-}C_2H_4)$ and C_2H_4 fragments in the product (*cis*-$W(CO)_4(\eta^2\text{-}C_2H_4)_2$) was calculated to be 48 kJ mol^{-1} which was much smaller than that of 122 kJ mol^{-1} in *trans*-$W(CO)_4(\eta^2\text{-}C_2H_4)_2$. In *cis*-isomer formation the strain along the reaction coordinate, $\Delta E_{strain}(\zeta)$, was always smaller than the accompanying stabilizing interaction ($E_{int}(\zeta)$).

Internal Excitation in the Product $W(CO)_4(\eta^2\text{-}C_2H_4)$ from C_2H_4 Coordination to $W(CO)_4$. The transient infrared absorption spectra observed following the pulse laser photolysis of gas phase $W(CO)_6$ in the presence of C_2H_4 showed a continuous band peak shift of the equatorial COs' vibration of $W(CO)_4(\eta^2\text{-}C_2H_4)$ in the region 1910–1930 cm^{-1} during C_2H_4 coordination to $W(CO)_4$ (0.8–2.4 μs under the total pressure of 6 Torr with balance Ar).[12,22] These time-resolved spectra are compared with calculated spectra showing the dependence of the CO vibration frequencies of $W(CO)_4(\eta^2\text{-}C_2H_4)$ on the angle β in Figure 5. The equatorial CO frequency increases with an increase in the angle β, while the axial one hardly depends on the angle. The nascent $W(CO)_4(\eta^2\text{-}C_2H_4)$ retains an internal energy of 125 kJ mol^{-1} originated from a W–C_2H_4 bond formation and is consequently relatively "hot". This means the C_2H_4 ligand is free to wag around the axis, as the energy even at β = 90° is higher than the lowest configuration ($\beta \approx 135°$) by only ca. 20 kJ mol^{-1} until collisional cooling takes effect. This axis is different from the principal axis of C_{2v} usually defined in group theory and passes roughly through CO_{ax}–W–CO_{ax} in the schematic structure **41-A**. A few microseconds seems to be required for the vibrational relaxation under the experimental conditions.

dx.doi.org/10.1021/ic300858d | *Inorg. Chem.* 2012, 51, 11365–11370

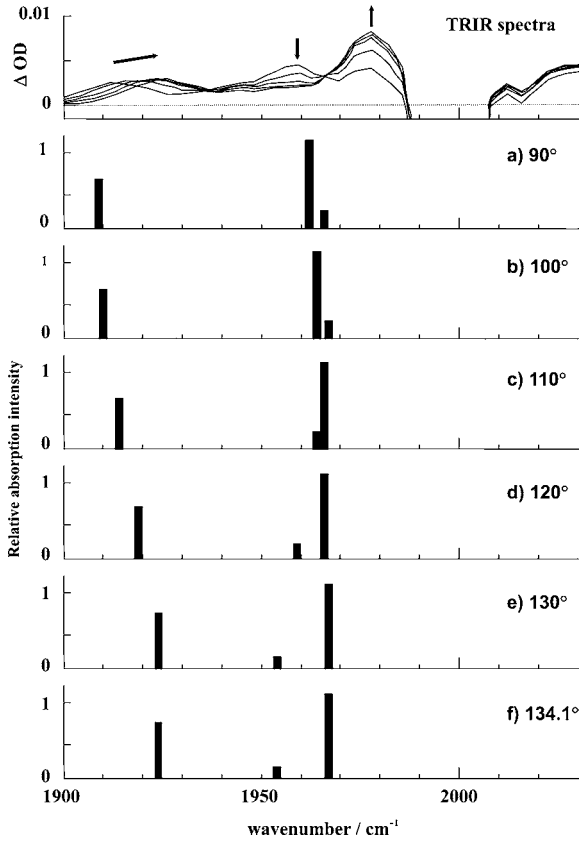

Figure 5. Dependence of the CO vibration frequencies on the ethene deformation angle β (90° (a) to 134.1° (f)) in $W(CO)_4(\eta^2\text{-}C_2H_4)$. Time-resolved infrared absorption spectra observed at 0.7 μs intervals over 0.8−2.4 μs after the 266 nm pulse laser photolysis of gas phase $W(CO)_6$ in the presence of C_2H_4 under the total pressure of 6 Torr with balance Ar are shown at the top. The TRIR spectra show the continuous band peak shift (right arrow) in the region 1910−1930 cm^{-1} corresponding to the change in the vibration frequency associated with the equatorial carbonyls in $W(CO)_4(\eta^2\text{-}C_2H_4)$ following C_2H_4 coordination on $W(CO)_4$. The decay of $W(CO)_4$ is shown by the down arrow, and the production of $W(CO)_4(\eta^2\text{-}C_2H_4)$ by up arrow.

Isomerizations of $W(CO)_4(\eta^2\text{-}C_2H_4)$ and $W(CO)_4(\eta^2\text{-}C_2H_4)_2$. Figure 6 shows the potential energy profile of the isomerization between the d-tbp $W(CO)_4(\eta^2\text{-}C_2H_4)$ (**41-A**) and the sp-apical $W(CO)_4(\eta^2\text{-}C_2H_4)$ (**41-C**). In this isomerization, there seems to be two main structural deformations. At first, a roughly 90° spin of C_2H_4 takes place accompanying a shift of C_2H_4 to the sp-basal position, and then the angle between two equatorial COs increases up to near 180°, resulting in the formation of sp-apical $W(CO)_4(\eta^2\text{-}C_2H_4)$ (**41-C**). The activation barrier was estimated to be ca. 100 kJ mol^{-1}. This fairly high barrier seems sufficient to inhibit d-tbp $W(CO)_4(\eta^2\text{-}C_2H_4)$ from isomerizing to sp-apical $W(CO)_4(\eta^2\text{-}C_2H_4)$ even though the nascent $W(CO)_4(\eta^2\text{-}C_2H_4)$ is formed in a hot state. This is consistent with the selective production of the d-tbp $W(CO)_4(\eta^2\text{-}C_2H_4)$ in the coordination reaction of C_2H_4 on $W(CO)_4$. In the square-pyramidal $W(CO)_4(\eta^2\text{-}C_2H_4)$, the apical−equatorial exchange (sp-basal ↔ sp-apical) does not occur through a tbp with C_2H_4 equatorial, although it might be expected in a Berry pseudorotation mechanism.

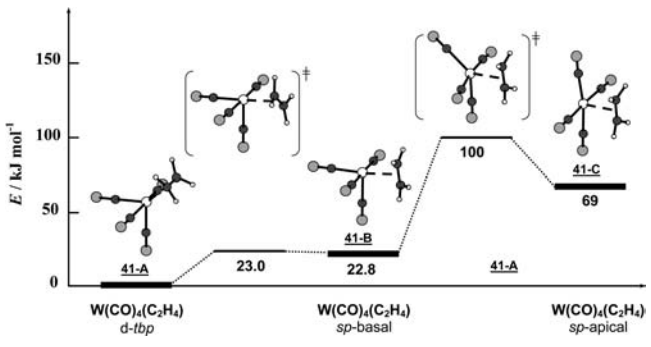

Figure 6. Schematic potential energy profile for the isomerization reaction between the d-tbp $W(CO)_4(\eta^2\text{-}C_2H_4)$ (**41-A**) and the sp-apical $W(CO)_4(\eta^2\text{-}C_2H_4)$ (**41-C**).

There is a high reaction barrier for the *cis*−*trans* isomerization of $W(CO)_4(\eta^2\text{-}C_2H_4)_2$, as shown in Figure 7. The *cis*-isomer ***c*-42-A** becomes ***c*-42-C** after sequential spins of approximately 90° of two ethenes, and it isomerizes to a *trans*-conformer across a reaction barrier of 126 kJ mol^{-1} through a transition state with trigonal-prismatic structure. With this fairly high barrier, it may be concluded that the *cis*−*trans* isomerization does not occur at room temperature.

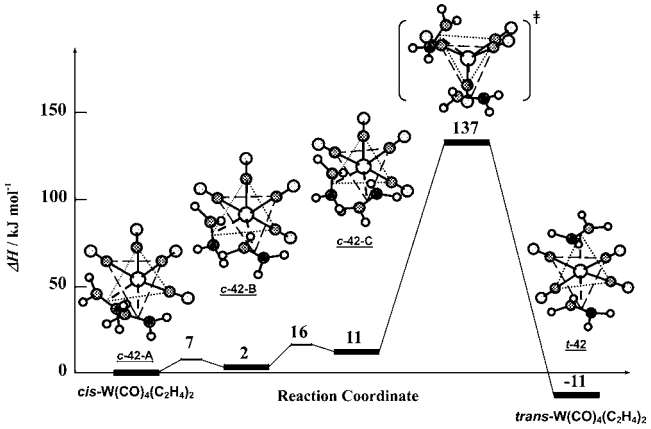

Figure 7. Schematic potential energy profile for the isomerization reaction between *cis*-$W(CO)_4(\eta^2\text{-}C_2H_4)_2$ (***c*-42-A**) and *trans*-$W(CO)_4(\eta^2\text{-}C_2H_4)_2$ (***t*-42**).

CONCLUSIONS

From a theoretical perspective there seems to be no possibility for the consecutive coordination of two ethenes on $W(CO)_4$ to result in *trans*-complex formation at room temperature. The primary coordination product, $W(CO)_4(\eta^2\text{-}C_2H_4)$, has a distorted-tbp structure with C_2H_4 equatorial (**41-A**), which is ca. 70 kJ mol^{-1} lower in energy than the sp structure with C_2H_4 apical (**41-C**). The isomerization from the distorted-tbp (**41-A**) to the sp (**41-C**) is inhibited because of the high activation barrier of ca. 100 kJ mol^{-1}. The second coordination results in the formation of *cis*-$W(CO)_4(\eta^2\text{-}C_2H_4)_2$ in a barrierless reaction, while a relatively high barrier of ca. 90 kJ mol^{-1} inhibits *trans*-$W(CO)_4(\eta^2\text{-}C_2H_4)_2$ formation. The *cis*-$W(CO)_4(\eta^2\text{-}C_2H_4)_2$ might be stable only at room temperature in the presence of excess C_2H_4 because the bond dissociation enthalpy of ca. 60 kJ mol^{-1} implies a dissociation lifetime of milliseconds. However, it seems to be impossible for *cis*-$W(CO)_4(\eta^2\text{-}C_2H_4)_2$ to isomerize to *trans*-$W(CO)_4(\eta^2\text{-}C_2H_4)_2$ on account of the high activation energy of ca. 140 kJ mol^{-1}.

dx.doi.org/10.1021/ic300858d | *Inorg. Chem.* 2012, 51, 11365−11370

■ ASSOCIATED CONTENT

Supporting Information

The three optimized structures, **41-A**, **41-B**, and **41-C**, for the singlet state of $W(CO)_4(\eta^2\text{-}C_2H_4)$ and the two optimized structures, ***t*-42** and ***c*-42-A**, in the lowest energy singlet states of *trans*- and *cis*-$W(CO)_4(\eta^2\text{-}C_2H_4)_2$. These data are available free of charge via the Internet at http://pubs.acs.org.

■ AUTHOR INFORMATION

Corresponding Author

*Fax: 81-(0)75-724-7580. E-mail: ishikawa@kit.ac.jp.

Notes

The authors declare no competing financial interest.

■ ACKNOWLEDGMENTS

The authors would like to thank Dr. D. M. Rayner at the National Research Council of Canada for his valuable discussion on transition-metal chemistry and Prof. Hisayoshi Kobayashi at Kyoto Institute of Technology for his fruitful discussion on quantum chemical calculations.

■ REFERENCES

(1) Cotton, F. A.; Wilkinson, G. *Advanced Inorganic Chemistry*; Wiley: New York, 1980.
(2) Stolz, I. W.; Dobson, G. R.; Sheline, R. K. *Inorg. Chem.* **1963**, *2*, 1264.
(3) Gregory, M. F.; Jackson, S. A.; Poliakoff, M.; Turner, J. *J. Chem. Soc., Chem. Commun.* **1986**, 1175.
(4) Grevels, F.-W.; Jacke, J.; Özkar, S. *J. Am. Chem. Soc.* **1987**, *109*, 7536.
(5) Perutz, R. N. *Chem. Soc. Rev.* **1993**, 361.
(6) Weiller, B. H.; Grant, E. R. *J. Am. Chem. Soc.* **1987**, *109*, 1252.
(7) Albright, T. A.; Hoffmann, R.; Thibeault, J. C.; Thorn, D. L. *J. Am. Chem. Soc.* **1979**, *101*, 3801.
(8) Albright, T. A.; Burdett, J. K.; Whangbo, M. H. *Orbital Interactions in Chemistry*; John Wiley & Sons: New York, 1985.
(9) Frenking, G.; Pidum, U. *J. Chem. Soc., Dalton Trans.* **1997**, 1653.
(10) Daniel., C.; Veillard, A. *Inorg. Chem.* **1989**, *28*, 1170.
(11) Daniel, C.; Veillard, A. *Nouv. J. Chim.* **1986**, *10*, 83.
(12) Takeda, H.; Jyo-o, M.; Ishikawa, Y.; Arai, S. *J. Phys. Chem.* **1995**, *99*, 4558.
(13) Frisch, M. J.; Trucks, G. W.; Schlegel, H. B.; Scuseria, G. E.; Robb, M. A.; Cheeseman, J. R. et al.*et al. Gaussian 03* (Revision B.05); Gaussian, Inc.: Pittsburgh, PA, 2003.
(14) Ishikawa, Y.; Kawakami, K. *J. Phys. Chem. A* **2007**, *111*, 9940.
(15) Kawakami, K.; Nakazawa, H.; Kinoshita, T.; Ishikawa, Y. *Bull. Chem. Soc. Jpn.* **2007**, *80*, 166.
(16) Andersson, M. P.; Uvdal, P. *J. Phys. Chem. A* **2005**, *109*, 2937.
(17) Foreman, J. B.: Frisch, A. *Exploring Chemistry with Electronic Structure Methods*; Gaussian, Inc.: Pittsburgh, PA, 1996; p 47.
(18) Ishikawa, Y.; Brown, C. E.; Hackett, P. A.; Rayner, D. M. *J. Phys. Chem.* **1990**, *94*, 2404.
(19) Herzberg, G. *Molecular Spectra and Molecular Structurwe III*; Krieger Publishing Company: Malabar, FL, 1991.
(20) Ishikawa, Y.; Hackett, P. A.; Rayner, D. M. *J. Phys. Chem.* **1988**, *92*, 3863.
(21) (a) Bickelhaupt, F. M. *J. Comput. Chem.* **1999**, *20*, 114. (b) Theodoor de Jong, G.; Bickelhaupt, F. M. *ChemPhysChem* **2007**, *8*, 1170. (c) van Zeist, W. -J.; Bickelhaupt, F. M. *Org. Biomol. Chem.* **2010**, *8*, 3118.
(22) Takeda, H.; Jyo-o, M.; Ishikawa, Y.; Arai, S. *Chem. Lett.* **1994**, 2287.